Electron Tomography

Second Edition

Electron Tomography

Methods for Three-Dimensional Visualization of Structures in the Cell

Second Edition

Joachim Frank
Editor

Springer

Joachim Frank
Wadsworth Center and
State University of New York
Albany, NY 10201
USA

Cover Illustration

Upper two panels: various topologies exhibited by the inner membrane of rat liver mitochondria. Chyong Ere Hsieh, Christian Renken, and Michael Marko, Resource for the Visualization of Biological Complexity, Wadsworth Center, Albany, New York. (Design: Michael Watters.)
Lower panel: principle of three-dimensional reconstruction from a tilt series. After Baumeister *et al*., Trends Cell Biol. 9 (1999) 81–85. (Design: Paxton Provitera and Michael Watters.)

Library of Congress Control Number: 200620791

ISBN-10: 0-387-31234-X Printed on acid-free paper
ISBN-13: 978-0387-31234-7

9 8 7 6 5 4 3 2 1

springer.com

Preface to the First Edition (1992)

Some physicists may be drawn to biology because of the challenge that lies in the vast complexity of biological matter; what attracted me initially was the curious paradox that makes electron microscopy of macromolecules possible—*phase contrast*, the contrast that arises not *despite* but *because* of, the imperfections of the objective lens. It is the capricious nature of such details that carries the promise of future problems finding totally unexpected (and sometimes surprisingly simple) solutions. Once engaged in electron microscopy, as a student I was in awe of the wide range of forms in which living matter is organized, but I was also frustrated by the central limitation of the instrument—that it renders these structures only in the confusing, highly ambiguous form of projections.

Three-dimensional information about an object is usually obtained in a cumbersome way, by a process that does not leave the object intact, namely by cutting and slicing, and by stacking or geometrically relating the resulting images. Consider the origins of anatomy, which set itself the task of making a three-dimensional image of the body with all its organs. It started as a heretical undertaking because it required dissection, intrusion into the body, violating its sancity which was being upheld by the Roman Church. Because of the need for dissection, the teaching of anatomy in the Middle Ages was a clandestine operation performed by candlelight in a windowless hall, with the corpse lying on a table that was specially designed to hide it rapidly, in case the authorities stormed the premises. Perspective anatomical drawings and three-dimensional models emerged as the result of an intense visual, tactile and visceral effort on the part of the scholar. Centuries after this type of three-dimensional imaging with the scalpel was begun, computerized axial tomography (CAT) was invented, a miraculous tool to look inside a living body without a single cut.

This book deals with a similar revolution (albeit on a different time scale) in the study of the cell's ultrastructure, brought about by the application of tomographic techniques to electron microscopy. For a long time, structural information about cell components had to be inferred from images of thin sections, the thickness being limited by the path length of 100-kV electrons in biological matter. The limitations of sectioning are well

known: it produces distortions and material loss, and additional errors arise in the attempt to stack the section images to form a three-dimensional representation. Organelles of complex shape have proved difficult or impossible to study in this way. The problem is solved by increasing the voltage to the range of 400 to 1000 kV, thereby increasing the penetration thickness, and using a *series of views* rather than a single one to generate a 'true' three-dimensional image. Again, an inside look is obtained into the structure, which remains intact during the investigation.

Similar techniques have been developed for macromolecular assemblies that are in a much smaller size range and require no increase in voltage. Thus, electron tomography has filled a large gap: for the first time, all hierarchies of structural organization, ranging from the level of atomic structure (explored by X-ray crystallography) to the architecture of the cell (explored by confocal scanning light microscopy) can now be studied by quantitative three-dimensional imaging techniques that require no symmetry or order. Although this book deals only with the mid-level of structural organization in this vast logarithmic range, the challenges posed by the explosive increase in the amount of data, and the need to make them accessible in some 'nested' way are becoming evident. Clearly, the revolution in the biology of the cell will not be complete until a system of data storage, retrieval and visualization is found that is capable of mapping out the intrinsic complexity of the cell's components—the cell as a walk-in world, one of the momentous challenges of computational biology.

This book emerged as the result of a long and sometimes tedious interaction with the contributors. I was lucky to find authors that were not only experts in their fields but also enthusiastic to cooperate and share my vision. I am very grateful for their patience and endurance. Special thanks go to Michael Radermacher and Bruce McEwen, who discussed with me the concept of the book. I also wish to acknowledge valuable suggestions by Pawel Penczek and Terry Wagenknecht, who helped me read and reconcile the contributions. Finally, I thank Amelia McNamara of Plenum for initiating an endeavor that allowed me to illuminate this stimulating topic from many directions.

Preface to the Second Edition

Electron tomography has come of age. The technique, which had long led an existence as a more or less esoteric exercise of a few determined groups, has largely become main-stream. Packaged software that can be bought with the electron microscope has alleviated the need for special training and has made electron tomography accessible to scientists with diverse backgrounds, including those with little or no background in mathematics, physics or computer science. High-visibility papers and reviews have appeared with stunning three-dimensional images depicting the organization of the cell or a particular organelle. In some cases, such as the mitochondrion, long-standing ideas about the architecture have turned out to be utterly false. As a result of this development, today's cell biologists confronted with vexing problems of spatial organization are more likely to consider an investment in 3D imaging. Depending on temperament, extent of funding and determination, this investment can take the form of collaboration with one of the existing NCRR/NIH-supported Biotechnology Centers, collaboration with a colleague in the same institution or an effort to install an electron microscope equipped with an automated tomography kit in their own laboratories.

The first edition of this book brought together a group of experts in the fundamental and practical aspects of the technique. While the material in the mathematically oriented chapters is still relevant, new ideas have emerged on how to optimize the results, and a literature has sprung up around the applications of the different approaches. Updated chapters by the original contributors will therefore be useful at this point. Additional mathematical/computational tools have gained importance, namely those that aid in the interpretation of the reconstructed volumes. Among these are techniques for denoising, segmentation, docking and fitting. I am grateful to all contributors for the great investment of time and effort they have put in this endeavor, not only in drafting their chapters, but also in helping me review all the material for consistency and accuracy.

Joachim Frank,
December 14, 2005

Contributors

Montserrat Bárcena • Universiteit Utrecht, Department of Molecular Cell Biology, Krupt Building, Room West 511, Padualaan 8, 3584 CH Utrecht, The Netherlands. m.barcena@bio.uu.nl

Sami S. Brandt • Helsinki University of Technology, Laboratory of Computational Engineering, PO Box 9203, FI-02015, Finland. Sami.Brandt@tkk.fi

Jose-Maria Carazo • Centro Nacional de Biotecnologia (CSIC), Universidad Autónoma, 28049 Cantoblanco, Madrid, Spain. carazo@cnb.uam.es

Achilleas S. Frangakis • EMBL, European Molecular Biology Laboratory, Meyerhofstr. 1, D-69117 Heidelberg, Germany. frangak@embl.de

Joachim Frank • Howard Hughes Medical Institute, Health Research, Inc. at the Wadsworth Center, Department of Biomedical Sciences, State University of New York at Albany, Empire State Plaza, Albany, NY 12201-0509, USA. Joachim@wadsworth.org

Peter W. Hawkes • CEMES-CNR, BP 94347, F-31055 Toulouse Cedex 4, France. hawkes@wanadoo.fr

Reiner Hegerl • Max Planck Institute for Biochemistry, Am Klopferspitz 18, D-82152 Martinsried, Germany. hegerl@ biochem.mpg.de

Gabor T. Herman • Department of Computer Sciences, The Graduate Center, City University of New York, New York, NY 10016, USA. gherman@gc.cuny.edu

Chyong-Ere Hsieh • Resource for Visualization of Biological Complexity, Wadsworth Center, Empire State Plaza, PO Box 509, Albany, NY 12201 USA. hsiehc@wadsworth.org

Qiang Ji • Electrical, Computer, and Systems Engineering Department, Rensselaer Polytechnic Institute, Troy, NY 12180, USA qji@ecse.rpi.edu

Ming Jiang • Electrical, Computer, and Systems Engineering Department, Rensselaer Polytechnic Institute, Troy, NY 12180, USA. qji@ecse.rpi.edu

Abraham J. Koster • Leiden University Medical Center, Molecular Cell Biology, Eindhovenweg 20, Leiden, The Netherlands. a.j.koster@lumc.nl

Jun Liu • Institute of Molecular Biophysics, Florida State University, Tallahassee, FL 32306-4380, USA. winker@bio.fsu.edu

Pradeep K. Luther • Imperial College, Biomedical Sciences Division, Sir Alexander Fleming Building, Exhibition Road, London SW7 2AZ, UK. p.luther@imperial.ac.uk

Carmen Mannella • Resource for Visualization of Biological Complexity, Wadsworth Center, Empire State Plaza, PO Box 509, Albany, NY 12201, USA. Carmen@wadsworth.org

Roberto Marabini • Escuela Politécnica Superior, Universidad Autónoma, 28049 Cantoblanco, Madrid, Spain. Roberto@cnb.uam.es

Michael Marko • Resource for Visualization of Biological Complexity, Wadsworth Center, Empire State Plaza, PO Box 509, Albany, NY 12201, USA. marko@wadsworth.org

David N. Mastronarde • The Boulder Laboratory for 3D Electron Microscopy of Cells, Department of Molecular, Cellular, and Developmental Biology, Campus Box 347, University of Colorado, Boulder CO 80309, USA. mast@colorado.edu

Bruce F. McEwen • Resource for Visualization of Biological Complexity, Wadsworth Center, Empire State Plaza, PO Box 509, Albany, NY 12201-0509, USA. bruce@wadsworth.org

Pawel A. Penczek • The University of Texas–Houston Medical School, Department of Biochemistry and Molecular Biology, 6431 Fannin, MSB 6.218, Houston, TX 77030, USA. Pawel.A.Penczek@uth.tmc.edu

Michael Radermacher • University of Vermont College of Medicine, Department of Molecular Physiology & Biophysics, HSRF Building, Rm 120, Burlington, VT 05405, USA. mraderma@physiology.med.uvm.edu

Bimal K. Rath • Wadsworth Center, Empire State Plaza, PO Box 509, Albany, NY 12201-0509, USA. bimal@wadsworth.org

Carlos O. S. Sorzano • Escuela Politécnica Superior, Universidad San Pablo–CEU, 28668 Boadilla del Monte, Madrid, Spain. Coss.eps@ceu.es

Kenneth A. Taylor • Institute of Molecular Biophysics, Florida State University, Tallahassee, FL 32306-4380, USA. taylor@bio.fsu.edu

Xun Wang • Electrical, Computer, and Systems Engineering Department, Rensselaer Polytechnic Institute, Troy, NY 12180, USA. qji@ecse.rpi.edu

Hanspeter Winkler • Institute of Molecular Biophysics, Florida State University, Tallahassee, FL 32306-4380, USA. winkler@bio.fsu.edu

Elmar Zeitler • Fritz-Haber-Institut der Max-Planck-Gesellschaft, Faradayweg 4–6, D-14195 Berlin, Germany. zr@fhi-berlin.mpg.de

Contents

Introduction: Principles of Electron Tomography

Joachim Frank

1. WHAT IS ELECTRON TOMOGRAPHY?

Tomography is a method for reconstructing the interior of an object from its projections. The word *tomography* literally means the visualization of slices, and is applicable, in the strict sense of the word, only in the narrow context of the single-axis tilt geometry: for instance, in medical computerized axial tomography (CAT-scan imaging), the detector–source arrangement is tilted relative to the patient around a single axis (Fig. 1a). In electron microscopy, where the beam direction is fixed, the specimen holder is tilted around a single axis (Fig. 1b). However, the usage of this term has recently become more liberal, encompassing arbitrary geometries, *provided that the specimen is actively tilted into multiple angles*. In line with this relaxed convention, we will use the term *electron tomography* for any technique that employs the transmission electron microscope to collect projections of an object that is tilted in multiple directions and uses these projections to reconstruct the object in its entirety. Excluded from this definition are 'single-particle' techniques that make use of multiple occurrences of the

Joachim Frank • Howard Hughes Medical Institute, Health Research, Inc. at the Wadsworth Center, Department of Biomedical Sciences, State University of New York at Albany, Empire State Plaza, Albany, NY 12201-0509, USA

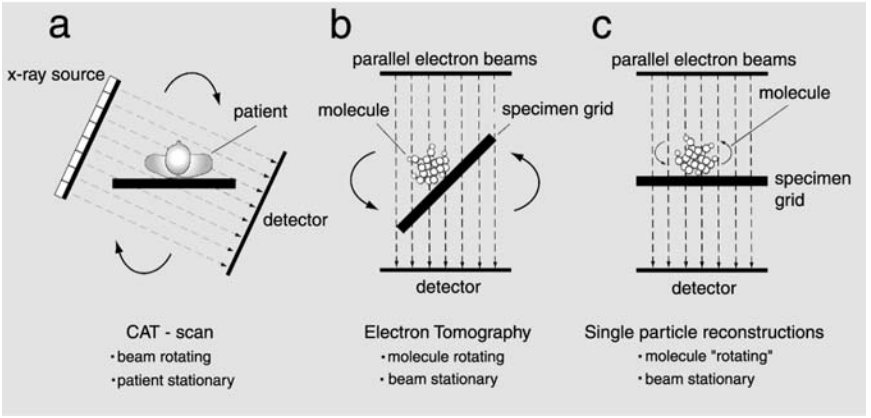

FIGURE 1. Three popular data collection geometries in 3D construction. (a) CAT-scan geometry, with the patient being stationary and a rigid source–detector arrangement tilted by equal increments; (b) equivalent single-axis tilt geometry in the transmission electron microscope, with the source–detector arrangement being stationary and the specimen tilted by equal increments; (c) as (b), but tilting replaced by the multiple incidence of molecules found in different random orientations.

object in different orientations, with or without the additional aid of symmetry (Fig. 1c). These techniques are covered elsewhere (non-symmetric: Frank, 1996, 2006; symmetric: Glaeser *et al*., 2007).

The terms '3D *imaging*' and '3D *electron microscopy*' have come into use as general terms to denote the capabilities of the instrument combined with the necessary computational tools to obtain a 3D image of an object's interior. For instance, a new series of Gordon Conferences was started in 1985 under the title 'Three-dimensional Electron Microscopy of Macromolecules', with the intention of providing a forum for scientists approaching the study of biological structure with both crystallographic and non-crystallographic techniques. (The term 3D *electron microscopy* may actually sound misleading since it conjectures an instrument with true 3D imaging performance. Such an instrument was actually conceived (Hoppe, 1972; Typke *et al*., 1976) but never advanced beyond the blueprint stage.)

2. A HISTORICAL PERSPECTIVE

3D imaging techniques are now commonplace in many areas of science, and it is difficult to recall that they have emerged only within the past 30 years; before that time, computers were simply too slow to be useful in processing 3D data on a routine basis, although much of the mathematical theory was well developed.

We may consider Plato's simile of the cave as a precursor to the reconstruction problem: here our ignorance of the essence of reality is depicted

by the situation of a man in a cave who watches shadows on the walls of his domicile; the shadows are all he sees of the world outside, and, because of the scantness of the information he receives, his comprehension of reality is severely limited. Similarly, a single projection, sometimes actually called a 'shadowgraph', of an object, is totally insufficient to establish its 3D shape. If we were prevented from changing the angle of view, we would be in a similar situation to the man in the cave, although without the dire existential ramifications.

The history of tomography (see also the brief account by Herman and Lewitt, 1979) is a history of intellectual challenges in a number of unrelated fields of science. As Elmar Zeitler recounts in Chapter 9, the same mathematical solution to the reconstruction problem that was found by Radon (1917) has had to be rediscovered numerous times. Two Nobel Prizes are directly related to 3D reconstruction: one that was shared by A. Cormack and G. N. Hounsfield in 1979 for the development of computerized axial tomography, and one in 1982 to Aaron Klug, in part for his pioneering work in the 3D reconstruction of molecular structures from their electron micrographs.

Klug traces the origins of 3D reconstruction in electron microscopy in his Nobel lecture (Klug, 1983). His laboratory, the Molecular Biology Laboratory of the Medical Research Council (MRC), is the appropriate starting point for a brief history of 3D imaging in electron microscopy. The predisposition of this institute for initiating quantitative structure research with the electron microscope is obvious, considering its historic role in the development of protein crystallography under Max Perutz's leadership.

DeRosier and Klug (1968) considered the problem of reconstructing the helical structure of the T4 phage tail from its projection (Fig. 2). To put their contribution into perspective, we must skip ahead and give a basic outline of the principle underlying 3D reconstruction. According to a fundamental mathematical theorem, the measurement of a projection yields a single central plane of the object's 3D Fourier transform. The Fourier transform, an alternative representation of the object, is a breakdown of the object's density distribution into sine waves. The Fourier transform constitutes a complete description of the object in the sense that, if we know the strengths (amplitudes) and phase shifts of all sine waves traveling in all possible directions and having wavelengths down to $d/2$, then the object is completely known to a resolution of d. The projection theorem thus suggests a recipe for reconstructing the object from its projections: by tilting the object through a range of $\pm 90^\circ$, we effectively sample its Fourier transform on a bundle of planes all intersecting one another on a single axis. It is clear that the angular spacing must be close enough to prevent information loss; in particular far away from the axis where the planes are maximally spaced and where the information on sine waves with the smallest wavelengths is situated.

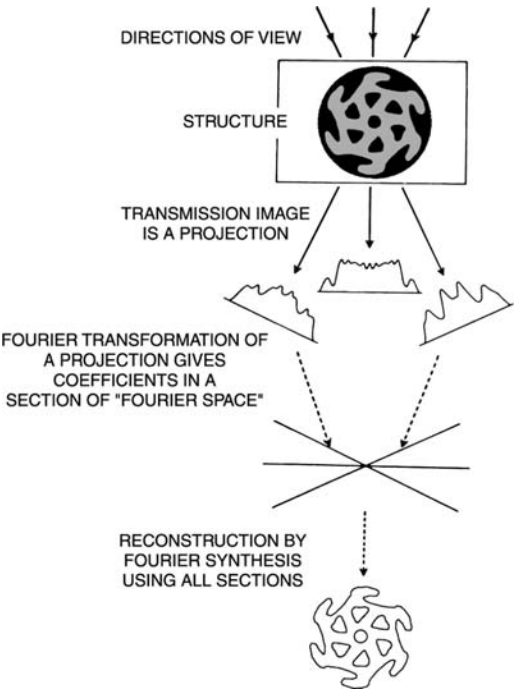

FIGURE 2. Principle of 3D reconstruction: the projections of the object furnish different central sections of the object's Fourier transform. If the number of projections is sufficient (making use of symmetries where possible), then the complete Fourier transform can be regenerated by interpolation, and from this the original object can be retrieved by inverse Fourier transformation. (Reproduced from DeRosier and Klug (1968), by permission of Macmillan Journals, Ltd.)

The application of this method to electron microscopy poses a problem because the tilt range is normally restricted for several reasons, the most important of which is the need to support the specimen on some type of grid that obstructs the electron path at high angles. Therefore, the angular range in commercial instruments does not usually exceed ±60°. Special tilt stages have been designed that push the range to ±85° (Chalcroft and Davey, 1984). However, when the object is contained in a thick plastic section, the increased path length of electrons traversing the sections at high angles also become a serious problem. One way to overcome this restriction is the development of tilt stages for cylindrical mounting of objects with 360° rotation capability. For instance, Barnard *et al.* (1992) placed a test object (spores) at the edge of an ultrathin glass capillary. Apart from these special cases, the experimental restriction to a range of about ±60° applies, which means that in the general case of an object without symmetry, a significant portion of the Fourier transform simply cannot be measured.

In contrast, when an object does possess symmetries, then the measurement of any projection yields other symmetry-related projections simultaneously. Another way of saying this is that, in this case, only part of the Fourier transform needs to be known for the entire Fourier transform to be generated. Among symmetric objects, those with helical symmetry, such as the T4 phage tail studied by DeRosier and Klug (1968), have a special position in that a single projection may be sufficient to generate the entire Fourier transform.

As early as 1970, Crowther and co-workers at the MRC formulated the approach to be used for reconstructing objects with or without symmetry with great clarity, and they also derived a general formula linking resolution, object size and number of projections. The first particle with icosahedral symmetry was reconstructed in 1970 (Crowther *et al.*, 1970b). Subsequently, Henderson and Unwin (1975) developed the reconstruction of single-layer, 'two-dimensional' crystals in the general crystallographic framework (see Amos *et al.*, 1982).

It is now necessary to illuminate the substantial contributions to the field by another group closely linked to crystallography: the group of Walter Hoppe at the Max Planck Institute in Munich (later relocated to Martinsried). Hoppe envisaged the prospect of 3D reconstruction in electron microscopy in imaging objects not amenable to crystallographic techniques. Consequently, he pursued almost exclusively the development of methods aimed at reconstructing objects lacking symmetry or crystalline order. Progress in this direction was initially slow because many tools of data processing had yet to be developed or adopted from other fields. The reconstruction of the fatty acid synthetase molecule in 1974 (Hoppe *et al.*, 1974) represented a significant achievement, which marked the beginning of electron tomography in the proper sense of the term. At that time, essentially all important tools were in place: the use of correlation functions for the alignment of projections, the Smith–Cormack scheme of 3D reconstruction (Cormack, 1964; Smith *et al.*, 1973) and the first sophisticated image-processing software system of modular design dedicated to electron microscopy applications (see Hegerl and Altbauer, 1982).

However, work in several other laboratories during that same period pointed to the deleterious effects of radiation damage, which made the quantitative interpretation of images taken with the standard imaging conditions questionable, and cast serious doubts on the significance of 3D information obtained by multiple exposure of the same object. According to Unwin and Henderson (1975), high-resolution information (at least to 7 Å) is preserved when the total dose is kept below 1 e/Å^2. Thus, it became apparent that 3D reconstruction would produce biologically significant results only under two rather narrowly defined circumstances: (i) when applied to macromolecular structures, only those data collection schemes are acceptable that make use of multiple occurrences of the same molecules, by extracting different projections from different 'repeats' of the molecule; and

(ii) when applied to cell components in an entirely different size range where resolution requirements are normally more modest (50–100 Å), and specialized higher voltage microscopes must be used for increased penetration, much higher accumulated radiation doses may be acceptable. In fact, these types of objects rarely exist in 'copies' with identical structure, thus excluding any approach that uses averaging implicitly or explicitly.

With hindsight, it must be seen as unfortunate that Hoppe's leading laboratory in 3D reconstruction of non-crystalline objects invested its main efforts in an area that does not fall in either category, namely tomography of single macromolecules (or complex assemblies such as the ribosome) from a tilt series, in the course of which the molecule receives a radiation dose that exceeds the limit found by Unwin and Henderson (1975) by a large factor. (The arguments put forward by Hoppe (1981) attempting to justify 3D electron microscopy of individual macromolecules receiving high doses of radiation are not convincing.)

Meanwhile, the general theory of 3D reconstruction was advanced by a number of studies; among these, the works of Bates's group (Lewitt and Bates, 1978a,b; Lewitt *et al*., 1978), Zwick and Zeitler (1973), Colsher (1977) and Gilbert (1972) should be mentioned for their relevance to our subject matter. 3D reconstruction in all areas of science proceeded at such a rapid rate that, in 1975, the Optical Society of America decided to organize a topical meeting on 3D reconstruction in Stanford, California. This meeting brought together contributors from a wide range of fields, such as geology, radioastronomy, radiology and electron microscopy. An overview of various implementations and applications presented at that meeting was compiled by Herman (1979).

At that time point, 3D reconstruction of general, asymmetric biological objects in electron microscopy took different paths, distinguished by the presence of redundancies or lack thereof, and the applicability of averaging techniques (Frank, 1975; Saxton and Frank, 1977). Particles, such as macromolecular assemblies, that exist in abundance with identical structure can be reconstructed from their 'single-particle' projections, i.e. from projections of particles that are dispersed and randomly oriented (Radermacher *et al*., 1987a,b; see Frank, 1996, 2006). Methods to align, classify and orient such projections, as well as 3D reconstruction from data with general geometries, constituted the main directions of algorithm development in this branch of 3D reconstruction. On the other hand, there are the kinds of specimen that lack redundancy altogether, and for such specimens—typically organelles and other subcellular structures—electron tomography is the only approach to 3D visualization available.

In the development of electron tomography of subcellular structures, progress hinged on the availability, to the biologist, of high- or intermediate-voltage electron microscopes equipped with precision tilt stages and supported by sophisticated image-processing resources. Centers with this degree of organization and sophistication did not emerge until the begin-

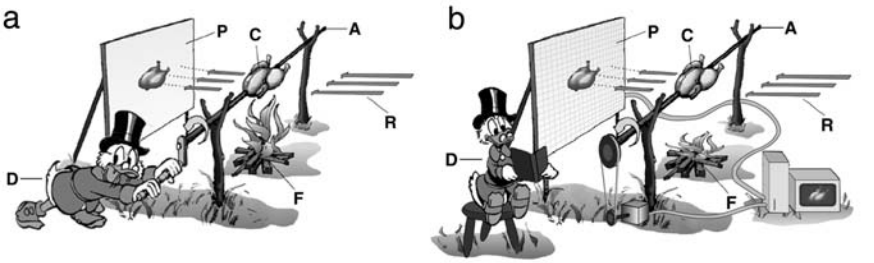

FIGURE 3. Electron tomography then (a) and now (b). (a) Adapted from Hoppe (1983); (b) adapted from B. Carragher, unpublished drawing.

ning of the 1980s when the National Institute of Health's Biotechnology program started to support three high-voltage microscopes dedicated to the biological sciences in the USA[1]. Thus, the pace of development of this technology was rather slow, especially considering the state of the art that already existed when Hoppe *et al*.'s fatty acid synthetase study (Hoppe *et al*., 1974) was published. However, perhaps the most important factor determining the pace with which 3D imaging with the electron microscope developed has been the speed and memory of computers. It must be realized that electron tomography posed computational problems of such magnitude that, until the beginning of the 1990s, only groups with access to mainframes were able to make significant progress. Other important factors were the slow progress toward automation of data collection and the need for image-processing software capable of handling the numerous combinations of operations that are encountered in the analysis of electron microscopic data.

Finally, the 1990s brought a breakthrough toward full automation, as affordable CCD cameras grew large enough to cope with the field sizes encountered in electron tomography, and electron microscopes were integrated with fast computer control. Here the work by Abraham Koster, one of the contributors to this volume (Chapter 4), deserves special mention (Koster *et al*., 1992). Nowadays, thanks to his and others' pioneering work, commercial instruments come equipped with the necessary gadgetry and software to perform low-dose data collection, as well as preliminary reconstruction, on the spot. Thus, with the new generation of powerful and smart electron microscopes, the drawing Walter Hoppe once used to illustrate both the potential (the capability of 3D imaging) and limitations (radiation damage) of electron tomography (Fig. 3a) has to be substantially revised (Fig. 3b).

[1] University of Colorado in Boulder, Colorado; University of Wisconsin in Madison; and New York State Department of Health in Albany, New York. Of these, only the one in Albany has remained in operation.

3. THE PRINCIPLE OF 3D RECONSTRUCTION

The principle of 3D reconstruction becomes clear from a formulation of the fundamental relationship between an object and its projections. An understanding of the basic concept of the Fourier transform is needed for this formulation. A brief introduction is provided in the following. For a more detailed introduction, the reader is referred to the specialized literature such as Bracewell (1999). A compilation of definitions and formulae for the case of discrete data is provided in the appendix of a book on 3D electron microscopy of macromolecular assemblies by the author (Frank, 2006).

The Fourier transform provides an alternative representation of an object by breaking it down into a series of trigonometric basis functions. For mathematical expediency, complex exponential waves of the form $\exp[2\pi i\mathbf{R}\mathbf{r}]$ are used instead of the more familiar sine and cosine functions. The argument vector describing a location in 3D space is $\mathbf{r} = (x, y, z)$, while $\mathbf{R} = (X, Y, Z)$ is a so-called spatial frequency vector, which gives both the direction of travel of a spatial wave and the number of full spatial oscillations per unit length. From such spatial waves, the object can be built up by linear superposition:

$$o(\mathbf{r}) = \sum_n c_n \exp[2\pi i\mathbf{R}_n\mathbf{r}] \tag{1}$$

with the complex coefficients c_n. The 3D Fourier transform may be visualized as a 3D scheme ('Fourier space') in which the coefficients c_n are arranged, on a regular grid, according to the position of the spatial frequency vector. Each coefficient c_n contains the information on the associated wave's amplitude (or strength),

$$a_n = |c_n| \tag{2}$$

and phase (or shift of the spatial wave in its travelling direction, with respect to the origin),

$$\phi_n = arctan\frac{Im\{c_n\}}{Re\{c_n\}} \tag{3}$$

The projection theorem offers a way to sample the Fourier transform of an object by measuring its projections. According to this theorem, *the 2D Fourier transform of a projection of the object is identical to a central section of the object's 3D Fourier transform.* Thus, by tilting the object into many orientations, one is, in principle, able to measure its entire Fourier transform. Obviously, the projections must be collected with a small angular increment and, ideally, over the full angular range. Then, after the Fourier summation in equation (1) is performed, the object can be retrieved. As always, the devil is in the details, as evidenced by the lengths and depths of the treatises by specialists found in this book.

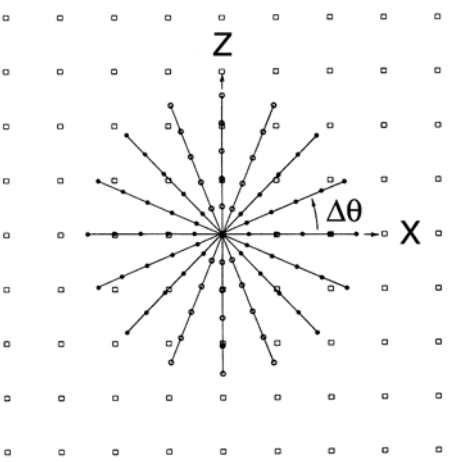

FIGURE 4. Sampling in Fourier space for single-axis tilting with equal increments $\Delta\theta$. For explanation, see text. Adapted from Frank (1992).

The angular increment $\Delta\theta$ is evidently determined by two parameters (Fig. 4): (i) the mesh size of the Fourier space grid; and (ii) the size of the region, in Fourier space, that needs to be filled. These quantities are in turn determined by object diameter and resolution:

1. The mesh size must be smaller than $1/D$, where D is the object diameter.
2. The region in Fourier space for which data must be acquired is a sphere with radius $1/d$, where d is the resolution distance, i.e. the size of the smallest feature to be visualized in the reconstruction.

According to these essentially geometrical requirements, the minimum number of (equispaced) projections works out to be (Bracewell and Riddle, 1967; Crowther *et al.*, 1970a):

$$N = \frac{\pi D}{d} \tag{4}$$

Reconstruction methods may be classified according to the way in which projections are collected or, alternatively, according to the way in which the object is retrieved from its measured projections. The former relates to the experiment, while the latter relates to the mathematical and computational aspects of reconstruction as discussed in Chapters 6, 7 and 8. As to the data collection geometries, there are three that have gained practical importance in electron microscopy: single-axis, double-axis and conical tilting.

Single-axis tilting is simply achieved by rotation of a side-entry rod in the electron microscope, whereas double-axis tilting involves a second tilt capability around an axis perpendicular to the first (Fig. 5a), and conical tilting provides a rotation capability in the inclined plane defined by the

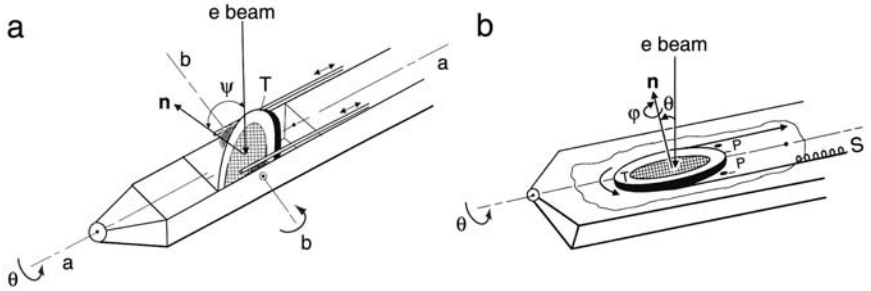

FIGURE 5. Schematic diagrams showing the principle of side-entry tilt stages with two degrees of freedom. (a) Double-tile stage. aa is the principal tilt axis, corresponding to the long axis of the rod. bb is the second tilt axis. θ and ψ are the corresponding tilt angles. **n** denotes the normal to the specimen plane. Tilting around the second axis is actuated by translation (indicated by arrows) of sliding rods which engage wheels attached to the turret T. (b) Tilt-rotation stage for conical geometry. Again **n** denotes the normal to the specimen plane. θ is the tilt angle, and φ the rotation angle in the plane of the circular turret T. Rotation is actuated by a cable pulled in the direction of the arrow, with return movement provided by a spring S. The turret is held in a stable position by retaining pins P. Adapted from Turner (1981).

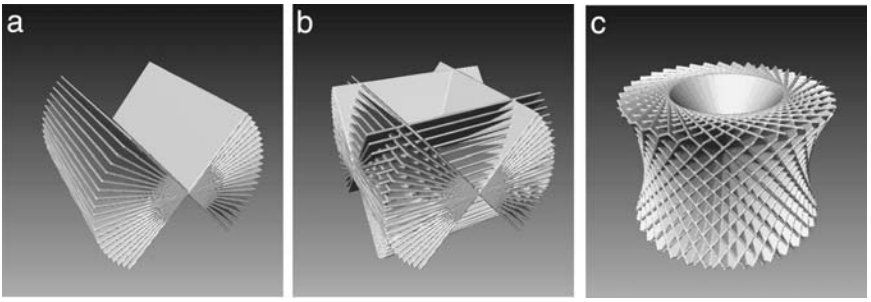

FIGURE 6. Coverage of 3D Fourier space in the case of three data collection geometries: (a) single-axis; (b) double-axis; and (c) conical. In each case, equal angular increments are depicted. From Lanzevecchia *et al.* (2005); reproduced with permission of Elsevier.

first tilt (Fig. 5b). It is easy to see, by invoking the projection theorem, that double-axis and conical tilting provide a much wider coverage of Fourier space if the maximum tilt angle is the same in all cases (Fig. 6a–c). However, the price to be paid for this information gain is a >2-fold increase in total dose (Frank and Radermacher, 1986; Radermacher and Hoppe, 1980). Because of this disadvantage, and the more elaborate experimental procedure, conical data collection has not been widely used in experimental protocols where a single biological structure is multiply exposed. (Conical data

collection, of course, has found widespread application in reconstructions of macromolecules in single-particle form from their projections (see Radermacher *et al*., 1987b).) Lately, the idea of using the conical tilt geometry in tomography has been revived by Lanzavecchia's group, with remarkable success (Lanzavechia *et al*., 2005; Zampighi *et al*., 2005).

4. HOW THIS BOOK IS ORGANIZED

The sequence of chapters in this book essentially follows the flow of information in electron tomography, proceeding from specimen preparation, to data collection in the instrument, and then to the techniques used for alignment, reconstruction and interpretation of the resulting tomographic volumes.

We start with the question of to what extent the object reconstructed from electron microscopic projections resembles the biological object. This question has three different aspects to it: one that has to do with the relationship between the native biological object and the specimen investigated in the electron microscope; the second with the relationship between that specimen and the images formed by the electron microscope; and a third with the relationship between the set of multiple projections and the final 3D image.

Two chapters deal specifically with the specimen preparation aspect and the question of fidelity to the original biological structure. The first, by Pradeep Luther (Chapter 1), examines the quality of specimen preparation in plastic sections, and the damage inflicted by the beam, with special attention to the problem of section shrinkage. Knowledge of the behavior of the specimen is of crucial importance in planning an experiment that requires multiple exposure of the same specimen. The other chapter, by Mike Marko, Chyongere Hsieh and Carmen Mannella (Chapter 2), describes experience gained with the new, promising technique of sectioning frozen-hydrated biological material prepared by high-pressure freezing for the purpose of electron tomography.

Peter Hawkes (Chapter 3) explores the conditions that must be satisfied in the imaging by electron microscopy for the observed projections to be regarded as simple line integrals of an object function. It is of course always possible to apply the reconstruction procedure 'blindly' to a set of experimental images and obtain a 3D density map, or 'object function'. The question is whether this reconstructed object has any meaning, or even a tractable relationship to the physical object the images originated from. By implication, the simple projection relationship and the image formation in bright field under the usual weak object assumptions yield a very elegant linear system description of the imaging and reconstruction process. As the specimen thickness increases, which is the case for cell sections investigated by electron tomography, multiple scattering increasingly interferes with the

linear system concept, but energy filtering (also covered in this chapter) can effectively increase the thickness range of validity.

Low-dose data collection, in the now common automated mode, is covered in a chapter by the pioneer of automated tomography, Abraham Koster, together with Montserrat Bárcena (Chapter 4). This chapter goes into all the necessary details regarding optimum settings, data collection protocols and the important considerations of dose fractionation.

Electron tomographic reconstruction requires that projections be aligned to a common frame of reference. The use of gold bead markers is now routine, and therefore it is justified that a chapter be devoted to the mathematical basis of marker-based alignment. David Mastronarde (Chapter 5), author of the well-known IMOD software, gives an expert introduction into this subject. However, the search for a reliable marker*less* alignment method continues, since the electron-opaque markers produce artifacts in the reconstruction volume that cannot be removed computationally. Sami Brandt (Chapter 6), one of the pioneers of markerless alignment techniques, has contributed an authoritative chapter on recent approaches to this problem.

Three chapters are devoted to the theory of reconstruction, addressing different issues that arise due to the peculiarities of data collection and numerical computation. We first present the chapter by Jose-Maria Carazo, Gabor Herman and co-workers (Chapter 7), which gives an overview on the approaches to the inverse problem presented by the reconstruction from a finite number of projections. This same chapter also introduces iterative algebraic methods, such as algebraic reconstruction techniques (ART) and related techniques. Next, Michael Radermacher (Chapter 8) goes into the details of weighted back-projection for general geometries, and formulates the algorithms underlying the computer programs now widely used in the field. Weighted back-projection methods have a special position in the practical implementation of 3D reconstruction, mainly because of their mathematical tractability and high computational efficiency. Radermacher summarizes the rationales and important formulae of weighted back-projection methods for regular and general geometries. Finally, in this section on the mathematics of reconstruction, Elmar Zeitler (Chapter 9) has contributed a chapter that presents an elegant general framework of reconstruction using special functions of mathematical physics, a chapter that brilliantly illuminates the inter-relationships of all approaches to reconstruction in use today.

Although the theoretical resolution obtainable in tomographic reconstructions is well known, the problem of how to measure the actual resolution achieved has been elusive. The chapter by Pawel Penczek and this author (Chapter 10) addresses this important issue with a new approach.

The remaining chapters in this book deal with different aspects of interpretation of the reconstruction. The first step is the removal of noise, either by simple Fourier filtration or more advanced "denoising" procedures. These procedures are described by Reiner Hegerl and Achilleas

Frangakis (Chapter 11). Segmentation is obviously the most important aspect as it is instrumental for the assignment of meaning to the different parts of a density map. Three chapters deal with segmentation, namely one authored by Achilleas Frangakis and Reiner Hegerl (Chapter 12), with segmentation based on local characteristics of the density distribution; the second, by Ming Jiang *et al*. (Chapter 13), on model-based segmentation making use of level set methods. The third chapter in this category addresses segmentation by rigid body motif search using cross-correlation. This chapter is co-authored by investigators who each have made separate contributions to this area of research: Achilleas Frangakis and Bimal Rath (Chapter 14). Another aspect of interpretation comes up when we try to characterize quasi-periodic structures, as presented by the complex organization of muscle trapped in the rigor state. We are then dealing with multiple versions of a 3D motif, which may allow the tracking of a physiological process evolving in time and space—a promising method of analysis described in the final chapter by Ken Taylor, Jun Liu and Hanspeter Winkler (Chapter 15).

ACKNOWLEDGEMENTS

This work was supported by HHMI and by Grant P41 RR01219 from the National Center for Research Resources (NCRR/NIH) and R37 GM 29169. I would like to thank Michael Watters for assistance with the illustrations.

REFERENCES

Amos, L. A., Henderson, R. and Unwin, P. N. T. (1982). Three-dimensional structure determination by electron microscopy of 2-dimensional crystals. *Prog. Biophys. Mol. Biol.* **39**: 183–231.

Andrews, H. C. (1970). *Computer Techniques in Image Processing*. Academic Press, New York.

Barnard, D. P., Turner, J.N., Frank, J. and McEwen, B.F. (1992). A 360° single-axis tilt stage for the high-voltage electron microscope. *J. Microsc.* **167**:39–48.

Bracewell, R. N. (1999). *The Fourier Transform and Its Applications*, 3rd edn. McGraw-Hill, New York.

Bracewell, R. N. and Riddle, A. C. (1967). Inversion of fan-beam scans in radio astronomy. *Astrophys. Soc*. **150**:427–434.

Chalcroft, J. P. and Davey, C. L. (1984). A simply constructed extreme-tilt holder for the Philips eucentric goniometer stage. *J. Microsc.* **134**:41–48.

Colsher, J. G. (1977). Iterative three-dimensional image reconstruction from tomographic projections. *Comput. Graphics Image Process.* **6**:513–537.

Cormack, A. M. (1964). Representation of a function by its line integrals, with some radiological applications. I. *J. Appl. Phys.* **35**:2908–2912.

Crowther, R. A., Amos, L. A., Finch, J. T. and Klug, A. (1970a). Three-dimensional reconstruction of spherical viruses by Fourier synthesis from electron micrographs. *Nature* **226**: 421–425.

Crowther, R. A., DeRosier, D. J. and Klug, A. (1970b). The reconstruction of a three-dimensional structure from projections and its application to electron microscopy. *Proc. R. Soc. B* **317**:319–340.

DeRosier, D. and Klug, A. (1968). Reconstruction of 3-dimensional structures from electron micrographs. *Nature* **217**:130–134.

Frank, J. (1975). Averaging of low exposure electron micrographs of nonperiodic objects. *Ultramicroscopy* **1**:159–162.

Frank, J. (1992). Introduction. In *Electron Tomography* (J. Frank, ed.) pp. 1–13. Plenum, New York.

Frank, J. (1996). *Three-dimensional Electron Microscopy of Macromolecules*. Academic Press, San Diego.

Frank, J. (2006). *Three-dimensional Electron Microscopy of Macromolecules*, 2nd edn. Oxford University Press, New York.

Frank, J. and Radermacher, M. (1986). Three-dimensional reconstruction of nonperiodic macromolecular assemblies from electron micrographs. In *Advanced Techniques in Electron Microscopy III* (J. K. Koehler, ed.). Springer-Verlag, New York, pp. 1–72.

Gilbert, P. F. C. (1972). The reconstruction of a three-dimensional structure from projections and its application to electron microscopy. II. Direct methods. *Proc. R. Soc. B* **182**:89–117.

Glaeser, R. M., Downing, K. H., Chiu, W., Frank, J. and DeRosier, D. (2007). *Electron Crystallography of Biological Macromolecules*. Oxford University Press, New York.

Hegerl, R. and Altbauer, A. (1982). The 'EM' program system. *Ultramicroscopy* **9**:109–116.

Herman, G.T. (ed.) (1979). *Image Reconstruction from Projections*. Springer-Verlag, Berlin.

Henderson, R. and Unwin, P. N. T. (1975). Three-dimensional model of purple membrane obtained by electron microscopy. *Nature* **257**:28–32.

Herman, G. T. and Lewitt, R. M. (1979). Overview of image reconstruction from projections, in *Image Reconstruction from Projections* (G. T. Herman, ed.). Springer-Verlag, Berlin, pp. 1–7.

Hoppe, W. (1972). Drei-dimensional abbildende Elektronenmikroskope. *Z. Naturforsch.* **27a**: 919–929.

Hoppe, W. (1981). Three-dimensional electron microscopy. *Annu. Rev. Biophys. Bioeng*. **10**: 563–592.

Hoppe, W. (1983). Elektronenbeugung mit dem Transmissions-Elektronenmikroskop als phasenbestimmendem Diffraktometer-von der Ortsfrequenzfilterung zur dreidimensionalen Strukturanalyse an Ribosomen. *Angew. Chem.* **95**:465–494.

Hoppe, W., Gassmann, J., Hunsmann, N., Schramm, H. J. and Sturm, M. (1974). Three-dimensional reconstruction of individual negatively stained fatty-acid synthetase molecules from tilt series in the electron microscope. *Hoppe-Seyler's Z. Physiol. Chem*. **355**:1483–1487.

Klug, A. (1983). From macromolecules to biological assemblies (Nobel lecture). *Angew. Chem.* **22**:565–636.

Koster, A. J., Chen, J. W., Sedat, J. W. and Agard, D. A. (1992). Automated microscopy for electron tomography. *Ultramicroscopy* **46**:207–227.

Lanzavecchia, S., Cantele, F., Bellon, P. L., Zampighi, L., Kreman, M., Wright, E., and Zampighi, G. A. (2005). Conical tomography of freeze-fracture replicas: a method for the study of integral membrane proteins inserted in phospholipids bilayers. *J. Struct. Biol*. **149**:87–98.

Lewitt, R. M. and Bates, R. H. T. (1978a). Image reconstruction from projections. I: General theoretical considerations. *Optik (Stuttgart)* **50**:19–33.

Lewitt, R. M. and Bates, R. H .T. (1978b). Image reconstruction from projections. III: Projection completion methods (theory). *Optik (Stuttgart)* **50**:189–204.

Lewitt, R. M., Bates, R. H. T. and Peters, T. M. (1978). Image reconstruction from projections. II: Modified back-projection methods. *Optik (Stuttgart)* **50**:85–109.

Radermacher, M. and Hoppe, W. (1980). Properties of 3D reconstruction from projections by conical tilting compared to single axis tilting. In *Proceedings of the 7th European Congress on Electron Microscopy*, Den Haag, Vol. I, pp. 132–133.

Radermacher, M., Wagenknechet, T., Verschoor, A. and Frank, J. (1987a). Three-dimensional structure of the large ribosomal subunit from *Escherichia coli*. *EMBO J*. **6**:1107–1114.

Radermacher, M., Wagenknecht, T., Verschoor, A. and Frank, J. (1987b). Three-dimensional reconstruction from single-exposure random conical tilt series applied to the 50S ribosomal subunit of *Escherichia coli*. *J. Microsc*. **146**:113–136.

Radon, J. (1917). Über die Bestimmung von Funktionen durch ihre Integralwerte längs gewisser Mannigfaltigkeiten. Berichte über die Verhandlungen der Königlich Sächsischen Gesellschaft der Wissenschaften zu Leipzig. *Math. Phys. Klasse* **69**:262–277.

Saxton, W. O. and Frank, J. (1977). Motif detection in quantum noise-limited electron micrographs by cross-correlation. *Ultramicroscopy* **2**:219–227.

Smith, P. R., Peters, T. M. and Bates, R. H. T. (1973). Image reconstruction from a finite number of projections. *J. Phys. A* **6**:361–382.

Turner, J. N. (1981). Stages and stereo pair recording. *Methods Cell Biol.* **23**:33–51.

Typke, D., Hoppe, W., Sessier, W. and Burger, M. (1976). Conception of a 3-D imaging electron microscopy. In *Proceedings of the 6th European Congress on Electron Microscopy* (D. G. Brandon, ed.), Vol. 1, Tal International, Israel, pp. 334–335.

Unwin, P. N. T. and Henderson, R. (1975). Molecular structure determination by electron microscopy of unstained crystalline specimens. *J. Mol. Biol*. **94**:425–440.

Zampighi, G., Zampighi, L., Fain., N., Wright, E. M., Cantele, F. and Lanzavecchia, S. (2005). Conical tomography II: a method for the study of cellular organelles in thin sections. *J. Struct. Biol*. **151**:263–274.

Zwick, M. and Zeitler, E. (1973). Image reconstruction from projections. *Optik* **38**:550–565.

1

Sample Shrinkage and Radiation Damage of Plastic Sections

Pradeep K. Luther

Pradeep K. Luther • Imperial College London, Biomedical Sciences Division, Sir Alexander Fleming Building, Exhibition Road, London SW7 2AZ, UK

1. INTRODUCTION

Just as fossil insects embalmed in amber are extraordinarily preserved, so are biological samples that have been embedded in plastic for electron microscopy. The success of embedding samples in plastic lies in the astounding resilience of the sections in the electron microscope, albeit after initial changes. The electron microscope image results from projection of the sample density in the direction of the beam, i.e. through the depth of the section, and therefore is independent of physical changes in this direction. In contrast, the basis of electron tomography is the constancy of the physical state of the whole section during the time that different views at incremental tilt angle steps are recorded.

The shrinkage of a plastic section in each dimension, especially the depth, when viewed in the electron microscope, is now a well known phenomenon. Knowledge of the shrinkage behavior of a section of a sample embedded in a particular plastic is of crucial importance when embarking on the electron tomography of the sample. In the last 15 years, the most important advances in electron tomography have been the development of automated methods of recording tilt series and direct imaging onto CCD cameras (Koster *et al*., 1997; Koster and Barcena, Chapter 4 in this volume). These advances have enabled tremendous savings in labor but also in the total dose experienced by a sample. In this chapter, we review the studies carried out on shrinkage behavior of samples embedded in various resins and we review the protocols that have been followed by the leading proponents of electron tomography.

2. ON RADIATION DAMAGE

Several researchers have written reviews on the effects of the electron beam on biological samples (Egerton *et al*., 2004; Glaeser and Taylor, 1978; Grubb, 1974; Lamvik, 1991; Reimer, 1989; Stenn and Bahr, 1970). Electron microscope radiation has the primary effect of producing intense ionization in organic materials, which results in the formation of free radicals and ions. This causes bond scission and molecular fragments to be formed. These primary effects occur at all temperatures. At room temperature, the free radicals and molecular fragments can undergo diffusion, and produce cross-

linking or further chain scission. Damage to secondary structure occurs at an electron dose of <100 e/nm^2. Further exposure causes the tertiary structure to undergo dramatic reorganization following loss of specific groups and altered structural composition. The dominant effect finally is that of mass loss from the sample, which preferentially involves H and O in comparison with C and N. The mass loss is accompanied or followed closely by shrinkage of the sample normal to the beam.

We can reduce the radiation damage on an organic sample by cooling the sample to cryotemperatures and by using low-dose techniques (to be described later). One of the main effects of electron irradiation at conventional illumination levels is to cause specimen shrinkage normal to the plane of the sample. The effect of the shrinkage in reciprocal space is illustrated in Fig. 1. The example considered is a structure based on cubic

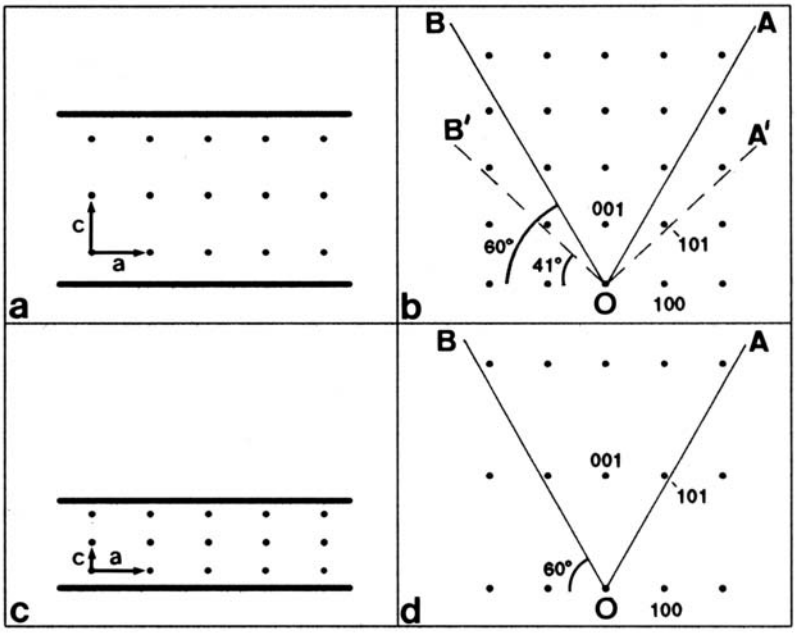

FIGURE 1. Illustration of the 'missing wedge' problem due to specimen shrinkage in the electron microscope. (a) Projection of a cubic crystal (for example) viewed edge-on with the *c* axis parallel to the electron beam. (b) Reciprocal lattice for the projection in (a). A conventional tilt holder in the electron microscope can be tilted in the range in the range of –60° to +60°. When a tilt series is recorded about a single tilt axis, and the 3D transform calculated by combining the individual transforms, data will be missing from the 3D transform inside the 'wedge' *AOB* of angle 60°. If the sample thickness reduces by 50% as in (c), then the corresponding reciprocal lattice shown in (d) is stretched 100% along *c**. The projection for the 101 diffraction spot, comfortably included in the tilt series for the unshrunk sample (a and b), now lies within the missing wedge. In relation to the original reciprocal lattice, the missing wedge is now described in (a) by *A*′*OB*′ and has an angle of 98°. For 50% shrinkage, the tilt holder effectively covers only the range –41° to +41° in relation to the original sample.

symmetry (Fig. 1a), which collapses in thickness by 50% (Fig. 1c). With a conventional tilt holder, a series of views about a single tilt axis are recorded in the range –60° to +60°. The 3D transform in (Fig. 1b), obtained by combining the transforms of the individual views, has missing from it data in the 60° wedge *AOB*. In the case of the 50% collapsed sample (Fig. 1c), the reciprocal space is stretched by 100% in the corresponding direction (Fig. 1d). The volume of the 3D transform that can be sampled is now much reduced, e.g. the spot 101 present in (Fig. 1b) is missing from the transform (Fig. 1d). In relation to the original sample, the missing wedge (*A′OB′*) in the 3D transform has an angle of 98°. The effective tilt range is now only ±41°. Sample shrinkage therefore directly reduces the resolution normal to the sample plane in a tomogram of a plastic-embedded sample. Hence we must make every effort to curtail the shrinkage.

It is appropriate to describe the terminology of Amos *et al.* (1982) for the various imaging modes in the electron microscope and the electron dose involved for a single image in each case. A dose on the sample of 50–400 e/nm^2 is considered as a *very low dose*, which is appropriate for very high resolution studies of unstained crystalline specimens. A dose of ~1000–2000 e/nm^2 is termed a *minimal dose*, which is used for stained or non-crystalline specimens. Conventional microscopy for single images involves doses on the order of ~5000–50,000 e/nm^2 due to the time involved in searching and focusing. Minimal and low-dose methods require a search of suitable areas to be done at very low magnification, about ×2000, during which the dose should be extremely low (~2 e/nm^2). Modern electron microscopes provide low-dose imaging modes in which the focusing is done at high magnification on areas adjacent to the area of interest, followed by image recording at the desired magnification.

3. ON SAMPLE PREPARATION

3.1. Fast Freezing/Freeze Substitution

To produce plastic-embedded samples with the best possible preservation, rapid freezing followed by freeze substitution has been the most successful method. Various methods have been used for rapid freezing. Sosa *et al.* (1994) successfully froze muscle fibers by ‘plunge-freezing’, which involves rapid propulsion of the sample into a trough of cold cryogen, e.g. liquid ethane, at –180°C. ‘Slam-freezing’ involves rapidly propelling a sample onto a highly polished metal block (usually copper) cooled by liquid helium or liquid nitrogen. Spectacular fast-freeze deep-etch replica images of various samples were obtained in the pioneering studies by Heuser (Heuser, 1989; Heuser *et al.*, 1987). Details of the slam-freezing method applied to striated muscle fibres to capture different activity states have been described (Craig *et al.*, 1992; Hirose *et al.*, 1993; Liu *et al.*, 2004a; Padron *et al.*, 1988).